

Cell and Organ Transplantation. 2023; 11(1): 34-45.
<https://doi.org/10.22494/cot.v11i1.148>

Human umbilical cord-derived mesenchymal stromal cells mitigate lipopolysaccharide-induced liver injury in rats



Redko O., Dovgalyuk A., Nebesna Z., Kramar S., Sverstyuk A., Korda M.

I. Horbachevsky Ternopil National Medical University, Ternopil, Ukraine

*Corresponding author's e-mail: dovgalyuk@tdmu.edu.ua

ABSTRACT

Acute Respiratory Distress Syndrome (ARDS) is a severe clinical condition that can cause multiple organ dysfunction, including liver injury. Human umbilical cord-derived mesenchymal stromal cells (hUC-MSCs) have been shown to possess therapeutic potential for a variety of diseases due to their ability to differentiate into various cell types and their anti-inflammatory and immunomodulatory properties.

THE PURPOSE. To investigate the potential of hUC-MSCs for treating lipopolysaccharide (LPS)-induced liver injury in rats.

MATERIALS AND METHODS. 72 mature male Wistar rats were randomly assigned to nine groups: control, 3 days, 7 days, and 28 days after intranasal administration of LPS, 24 hours of LPS and 2 days of hUC-MSCs, 4 days of LPS and 3 days of hUC-MSCs, 14 days of LPS and 14 days of hUC-MSCs, 21 days of LPS and 7 days of hUC-MSCs injection, and control 3 days after hUC-MSCs injection. The isolation of MSCs from human umbilical cord tissue was performed using an enzymatic digestion method with collagenase I. hUC-MSCs were injected intraperitoneally at a dose of $1 \cdot 10^6$ cells/kg body weight. Serum levels of alanine aminotransferase (ALT), aspartate aminotransferase (AST) and alkaline phosphatase (ALP) were measured using the kinetic method. The levels of hepatocellular necrosis, liver structural damage, hepatocyte vacuolation, inflammation and disseminated intravascular coagulation (DIC) were analyzed by histological scoring of sections stained with hematoxylin and eosin. The expression of TGF- β 1 in the liver tissue was evaluated by immunohistochemistry.

RESULTS. The preclinical study demonstrated that treatment with hUC-MSCs significantly improved liver function and attenuated LPS-induced liver injury in rats. This was evidenced by a reduction in hepatocellular necrosis, liver structural damage, hepatocyte vacuolation, inflammation, signs of DIC, fibrosis and lower levels of serum liver markers ALT, AST and ALP in the hUC-MSCs-treated groups compared to the untreated groups. The study also revealed that the use of hUC-MSCs was more effective at the earlier stage of liver injury.

CONCLUSION. Our findings suggest that hUC-MSCs therapy may hold promise as a potential treatment for LPS-induced liver injury. Further research is needed to better understand the underlying mechanisms and to determine the potential for hUC-MSCs therapy in clinical practice.

KEY WORDS: liver injury; human umbilical cord-derived mesenchymal stromal cells (hUC-MSCs); cell therapy; histological analysis

Acute respiratory distress syndrome (ARDS) is a life-threatening condition that occurs in critically ill patients and is characterized by severe hypoxemia, diffuse lung infiltrates on chest radiographs, and respiratory failure [1-4]. ARDS has significant morbidity rates, and it remains a clinical challenge for healthcare providers worldwide. Despite advances in understanding its pathophysiology and management, ARDS continues to be associated with high rates of mortality, ranging from 35 to 46 % [5].

ARDS is a serious condition that can have far-reaching effects beyond the lungs. ARDS is known to cause multiple organ dysfunction syndrome, which can result in the failure of various organs, including the liver. The liver plays a crucial role in metabolic processes and detoxification, and

its dysfunction can have serious implications for patient outcomes. In patients with ARDS, liver dysfunction is a common complication that can contribute to the overall severity of the illness. In spite of the advances in supportive care, treatment options for ARDS-induced liver injury are limited [6, 7].

Hepatocellular hypoxia, a condition characterized by insufficient oxygen supply to the liver cells, is a major contributor to liver injury in ARDS. During ARDS, the lungs become damaged, leading to reduced oxygen supply to the body's organs, including the liver. The liver is particularly susceptible to hypoxia due to its high metabolic demands and limited oxygen reserve capacity. Hepatocytes exposed to hypoxia undergo a range

of cellular changes, including a reduction in mitochondrial respiration and an increase in anaerobic glycolysis. As a result, the liver's energy supply becomes compromised, leading to the death of hepatocytes. This process can also lead to the release of inflammatory cytokines, further exacerbating liver injury. The death of hepatocytes due to hepatocellular hypoxia highlights the importance of preserving liver function during the course of ARDS [8, 9].

During ARDS the liver is subjected to the effects of systemic inflammation, which can lead to liver injury and dysfunction. The inflammatory response that occurs during ARDS involves the release of cytokines and other pro-inflammatory mediators that can damage hepatocytes and promote liver inflammation. This can result in changes in liver function, including alterations in the metabolism and clearance of drugs, as well as the production of liver enzymes and other markers of liver damage [10-12].

The liver is also involved in the clearance of inflammatory mediators from the circulation. This process can become overwhelmed during ARDS, leading to the accumulation of pro-inflammatory cytokines in the systemic circulation and exacerbating the inflammatory response. In addition, the liver is an important site of immune cell activation and recruitment, and the dysregulation of immunocyte function during ARDS can contribute to liver injury and inflammation. Overall, the impact of the systemic inflammatory response during ARDS on the liver is complex and multifactorial, involving both direct and indirect effects on liver function and integrity [13-17].

The use of lipopolysaccharide (LPS) for modeling ARDS in rats has been well-established and widely adopted. LPS, a component of the outer membrane of Gram-negative bacteria, is known to induce a robust inflammatory response and mimic the pathophysiological features observed in human ARDS. Its ability to activate toll-like receptor 4 signaling pathway triggers the release of pro-inflammatory cytokines, such as tumor necrosis factor-alpha, interleukin-1 beta, and interleukin-6, leading to pulmonary inflammation and injury. The administration of LPS to rats allows for the reproducible induction of ARDS-like symptoms, including increased pulmonary vascular permeability, infiltration of inflammatory cells, alveolar edema, and impaired oxygenation [18-22].

One of the advantages of human umbilical cord-derived mesenchymal stromal cells (hUC-MSCs) is that these cells can be easily obtained from the perinatal material, which is usually discarded after birth. Compared to other types of stem cells, such as embryonic stem cells or induced pluripotent stem cells, these MSCs have a lower risk of tumorigenesis and do not raise ethical concerns [23; 24].

In addition, hUC-MSCs have been shown to have a low immunogenicity and can exert their therapeutic effects without eliciting an immune response, making them suitable for allogeneic transplantation. This feature makes hUC-MSCs therapy a potentially attractive option for the treatment of a wide range of diseases [23-26].

In this study, we sought to research the ability of hUC-MSCs to treat liver injury induced by LPS in rats. Our findings provide insight into the potential of hUC-MSCs therapy for the treatment of liver injury, associated with ARDS, and offer a basis for further investigation of this therapeutic approach.

MATERIALS AND METHODS

Animals. 72 mature white male Wistar rats weighting 200-220 g were used in this study. Rats were housed in a temperature-controlled room with a 12-hour light/dark cycle and had free access to water and food. All animal experiments were conducted in accordance with the provisions of the European Convention for the Protection of Vertebrate Animals used for Experimental Purposes (Strasbourg, 1986; Oslo, 2018) and the Law of Ukraine #3447-IV "On Protection of Animals from Cruelty" (dated 21.02.2006). The study was approved by the Bioethics Commission of Ternopil National Medical University, protocol #60, dated 01.09.2020.

Experimental design. Rats were randomly divided into nine groups (n = 8 per group):

- 1) control – normal rats;
- 2) 3d of LPS – 3 days after LPS administration;
- 3) 7d of LPS – 7 days after LPS administration;
- 4) 28d of LPS – 28 days after LPS administration;
- 5) 24h of LPS and 2d of hUC-MSCs – rats which received hUC-MSCs injection 24 hours after LPS and were sacrificed 2 days afterwards;
- 6) 4d of LPS and 3d of hUC-MSCs – rats which received hUC-MSCs injection 4 days after LPS and were sacrificed 3 days afterwards;
- 7) 14d of LPS and 14d of hUC-MSCs – rats which received hUC-MSCs injection 14 days after LPS and were sacrificed 14 days afterwards;
- 8) 21d of LPS and 7d of hUC-MSCs – rats which received hUC-MSCs injection 21 days after LPS and were sacrificed 7 days afterwards;
- 9) control hUC-MSCs – intact rats sacrificed 3 days after hUC-MSCs injection.

LPS from *E. coli* (*Sigma-Aldrich*, USA) was administered intranasally at a dose of 5 mg/kg.

Cryopreserved hUC-MSCs were generously provided by Prof. Lavrenchuk H. Y. from the Medical Center Phoenix, Bulgaria. Umbilical cord tissue was obtained from a single donor following normal childbirth according to informed consent. Under aseptic condition, the umbilical cord tissue was dissected into small fragments and subjected to enzymatic digestion using a 0.1 % collagenase I (*Sigma-Aldrich*, USA), diluted in DMEM/F12 Advanced culture medium (*Gibco*, USA). Cell suspension was then pipetted and centrifuged for 5 minutes at 1610×g. The resulting pellet was resuspended in culture medium supplemented with 10 % fetal bovine serum (FBS) (*Gibco*, USA) and seeded into culture flasks. The isolated hUC-MSCs were cultured in a controlled incubation environment at a temperature of 37 °C and a CO₂ concentration of 5 %. The obtained primary cultures were assigned as passage 0 (P0). Passaging was performed using trypsinization with TrypLE Express Enzyme (*Gibco*, USA) upon reaching 90-100 % confluence. Cryopreservation was performed at passage 4 after reaching 90 % confluence. For cryopreservation, 50 % of the cell suspension (2·10⁶ cells) in DMEM culture medium was added to cryovials. Then, freezing medium containing 30 % DMEM/F12 Advanced, 40 % FBS, 20 % conditioned medium and 10 % dimethyl sulfoxide (*Sigma*, USA) was added in two steps. Further storage was carried out at -80 °C (intermediate stage) and in liquid nitrogen at -196 °C.

The obtained hUC-MSCs were subjected to immunophenotyping by flow cytometry using a BD Accuri™ C6 Plus Personal Flow Cytometer (*Becton Dickinson*, USA), as well as mouse anti-human monoclonal antibodies against CD73, CD90, CD105, CD34, and CD45 (*Invitrogen*, USA). hUC-MSCs were characterized as CD73⁺, CD90⁺, CD105⁺, CD34⁻, CD45⁻. After thawing, hUC-MSCs were cultured using Advanced DMEM/F12 medium (*Gibco*, USA), supplemented with 10 % FBS, 1 % L-Glutamine-Penicillin-Streptomycin solution (*Sigma*, USA) and 240 µg/L heparin (*Sigma*, USA). The cells were cultured in a controlled environment at 5 % CO₂ and a temperature of 37 °C. For the experimental procedures, MSCs at passage 5 were used.

hUC-MSCs were administered via intraperitoneal injection, resuspended in 0.25 mL of saline solution at a dose of 1·10⁶ cells/kg body weight. The dose of hUC-MSCs was selected based on previous studies that have used the same dosage [29-32]. The intraperitoneal route of hUC-MSCs administration was chosen because of the fact that intraperitoneal injection results in higher cell retention in the peritoneal cavity, allowing for prolonged exposure of MSCs to the local microenvironment [33]. Therefore, MSCs injected intraperitoneally can exert their therapeutic effects locally within the peritoneal cavity, which is beneficial for liver injury. In addition, intraperitoneal injection has a lower risk of embolism and is easier and less technically challenging compared to intravenous injection in rats. Animals were not immunosuppressed following the administration of hUC-MSCs injections, as these stem cells are known to elicit minimal or no immune response [23-26].

In order to correctly evaluate the effectiveness of different times of MSC treatment, the data was divided into 3 comparison groups:

- 1) control, 7d, 4d LPS + 3d hUC-MSCs and control hUC-MSCs (3d);
- 2) control, 3d and 24h LPS + 2d hUC-MSCs;
- 3) control, 28d, 14d LPS + 14d hUC-MSCs and 21d LPS + 7d hUC-MSCs.

These time points were strategically chosen to correspond to different stages of ARDS [27; 28]. It was previously identified that three stages of ARDS in rats are exudative (6-24 hours), fibroplasia (3-7 days) and fibrosis (14-28 days) (the data are being prepared for publication). In groups 5-8, the animals were sacrificed at different time points following hUC-MSCs injections (2 days in group 5, 3 days in group 6, 14 days in group 7, and 7 days in group 8) to enable a comparative analysis with the corresponding groups that did not receive hUC-MSCs treatment. Animals in group 9 were sacrificed 3 days after hUC-MSCs injection in order to observe the mid-term action of hUC-MSCs.

Terminal anesthesia was performed with a lethal dose of sodium thiopental (150 mg/kg) injected intraperitoneally. At the time of sacrifice, blood and liver samples were collected for further analysis. Blood samples were collected from each rat through cardiac puncture. Serum levels of alanine aminotransferase (ALT), aspartate aminotransferase (AST) and alkaline phosphatase (ALP) were measured using the kinetic method. The measurements were performed using a semi-automatic biochemistry analyzer Master T (*Hospitex*, Italy) and commercial kits (*Spinreact*, Spain) following the manufacturer's instructions.

Liver samples were immediately fixed in 10 % neutral buffered formalin. The fixed liver tissues were then processed using a tissue processor LOGOS One (*Milestone Medical*, USA) following standard protocols and embedded in paraffin wax. 5 μ m thick sections were obtained using a rotary microtome AMR 400 (*Amos scientific*, Australia).

To visualize the tissue morphology and the extent of liver injury, the sections were stained with hematoxylin and eosin (H&E). A total of 72 paraffin blocks were prepared for histological and immunohistochemical studies. On average, three liver fragments were embedded in each block. Two serial sections were mounted on glass slides for histological analysis. Following the analysis of the sections stained with hematoxylin-eosin, subsequent steps involved the preparation of slides specifically for immunohistochemical investigation. One section from each block was mounted on a glass slide. All sections were analyzed, with approximately 200 sections for histological and approximately 100 sections for immunohistochemical studies. All samples were examined under a light microscope Eclipse Ci-E (*Nikon*, Japan) and documented using a camera M3CMOS 14000 (*Sigeta*, Ukraine) and a TouP View software (*TouPtek Photonics*, China).

Immunohistochemistry was performed to evaluate the expression of transforming growth factor-beta 1 (TGF- β 1) in the liver tissue samples. Paraffin-embedded tissue sections were deparaffinized, rehydrated, and subjected to heat-induced antigen retrieval. Endogenous peroxidase activity was blocked using 3 % hydrogen peroxide. Recombinant rabbit monoclonal primary antibodies to TGF- β 1 (Cat. No. ab215715, Abcam, USA), and detection system Mouse/Rabbit PolyVue™ HRP/DAB (*Diagnostic BioSystems*, USA), were used to detect TGF- β 1. The sections were counterstained with Mayer's hematoxylin.

The assessment of liver injury was conducted using a customized histological scoring system, developed by us, which included the evaluation of hepatocellular necrosis, liver structural damage, hepatocyte vacuolation, inflammation, signs of disseminated intravascular coagulation (DIC), and TGF- β 1 expression, measured through the means of immunohistochemistry. Hepatocellular necrosis was defined as the presence of areas of dead hepatocytes, characterized by pyknotic nuclei. Inflammation was assessed by the presence of infiltrating inflammatory cells in the liver, including lymphocytes, and neutrophils. Each histological parameter was assigned a score ranging from 0 to 3, with 0 indicating no damage and 3 indicating severe damage. The scoring for each parameter was then averaged among the 8 animals in each experimental group. Subsequently, the individual scores for all parameters were summed to calculate a total histological score ranging from 0 to 18, with higher scores reflecting more pronounced liver injury.

Statistical analysis. The collected data were analyzed using Statistica 10.0 (*Statsoft Inc.*, USA). Specifically box plots were used to visualize the data. The Kruskal-Wallis test was used to assess differences between the obtained data. $P < 0.05$ was considered statistically significant.

To determine the applicability of parametric or non-parametric statistical tests, the input data were tested for conformity to a normal distribution of research results. It was found that the input data did not follow a normal distribution. This is further supported by the values of skewness and kurtosis coefficients, as well as the small number of sampling points. In this case, we applied the non-parametric Kruskal-Wallis test, which allowed us to answer the question of whether the nominal multilevel factor (different time points) influences the quantitative response (ALT, AST and ALP concentrations) and whether the quantitative factor influences the nominal multilevel response. The basic data used were the concentrations of ALT, AST and ALP measured at different time points after LPS exposure and use of hUC-MSCs. Changes in ALT, AST and ALP concentrations are presented in two-dimensional graphs with box plots. Box plots on two-dimensional graphs are asymmetric, medians are not centered, thus providing additional evidence of the non-normal distribution of experimental data.

RESULTS AND DISCUSSION

The liver tissue of the intact rats (**Fig. 1 A**) and the rats of the hUC-MSCs control group (**Fig. 1 F**) showed no structural changes, with liver lobules composed of hepatocytes arranged in the shape of polygonal prisms.

Conversely, the liver of the rats three days after LPS exposure contained signs of hepatocyte degeneration with pyknotic nuclei and vacuolated cytoplasm. There were dark and light types of hepatocytes present, presumably due to their different functional states: the darker, more basophilic hepatocytes being generally more active and involved in metabolic processes, while the lighter hepatocytes were believed to be either damaged or less active (**Fig. 1 B**). In addition, there were signs of inflammation which manifested as a perivascular leukocyte infiltration, dilated and blood-filled vessels, and changes in the trabecular liver structure.

On the 7th day after LPS exposure, the liver still contained blood-filled vessels, pyknotic cells, and groups of lighter hepatocytes with more heterochromatic nuclei (**Fig. 1 C**). Leukocyte infiltration of the large vessels was still visible.

On the 28th day after LPS exposure, the area of vacuolated hepatocytes with destroyed nuclei was significantly increased. Lymphocyte infiltration of the large vessels was still present (**Fig. 1 D, E**).

The presence of thrombi in the liver vessels is a strong indicator of DIC, which is a serious and potentially fatal condition characterized by the widespread formation of blood clots in small blood vessels throughout the body. DIC is often a complication of systemic infections, trauma, cancer, or other underlying medical conditions, and it can lead to organ failure, hemorrhage, and death if not promptly diagnosed and treated.

In the context of ARDS, the development of DIC is not uncommon, as the systemic inflammation and tissue damage caused by the disease can trigger the coagulation cascade and lead to the formation of thrombi in the liver, lungs, and other organs. The presence of thrombi in the liver vessels in our study is consistent with the previous reports of DIC in ARDS patients, and it underscores the importance of monitoring coagulation parameters and treating DIC aggressively in critically ill patients with ARDS [5, 34-36].

To assess the effectiveness of hUC-MSCs treatment, we compared the liver tissue of untreated rats with that of rats treated with hUC-MSCs. On the 3rd day of LPS, the untreated liver (**Fig. 1 B**) showed dilated and blood-filled vessels which were not present in the treated liver (**Fig. 1 G**). The same was observed on the 7th day, with blood-filled vessels present in the untreated liver (**Fig. 1 C**) and none in the treated liver (**Fig. 1 H**). On the 28th day after LPS exposure, the untreated liver (**Fig. 1 D, E**) contained

vacuolated hepatocytes with destroyed nuclei, while the liver treated on the 14th day (**Fig. 1 I**) contained none of these.

We also analyzed the efficacy of hUC-MSc treatment at different times after LPS exposure. We found that the treatment at the earlier stage on the 14th day (**Fig. 1 I**) was more effective than at the later stage on the 21st day (**Fig. 1 J**), as evidenced by the liver's superior condition with fewer signs of damage and inflammation as well as the absence of blood clots in liver vessels.

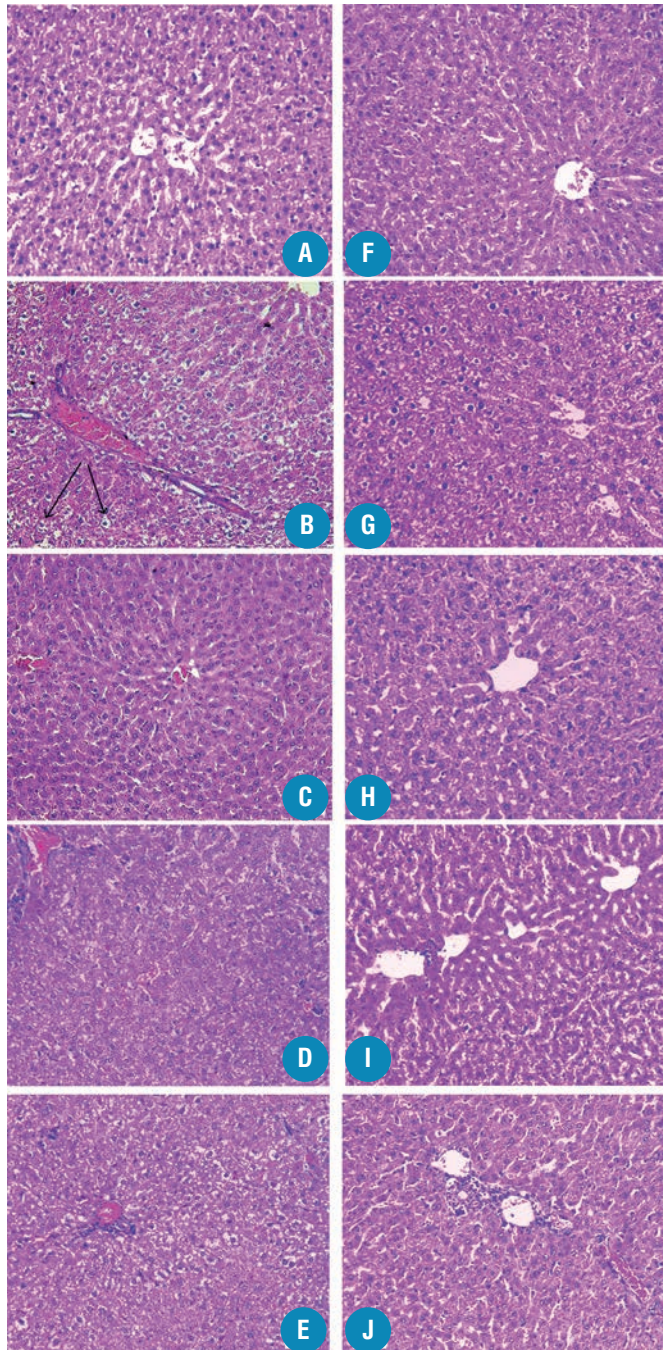


Fig. 1. Representative samples of rat liver histological sections of control (A), 3d of LPS (B), 7d of LPS (C), 28d of LPS (D and E), control hUC-MSCs (F), 24h of LPS and 2d of hUC-MSCs (G), 4d of LPS and 3d of hUC-MSCs (H), 14d of LPS and 14d of hUC-MSCs (I), and 21d of LPS and 7d of hUC-MSCs (J) groups. Arrows point at damaged hepatocytes with piknotic nuclei. H&E staining; images were captured at 200x magnification.

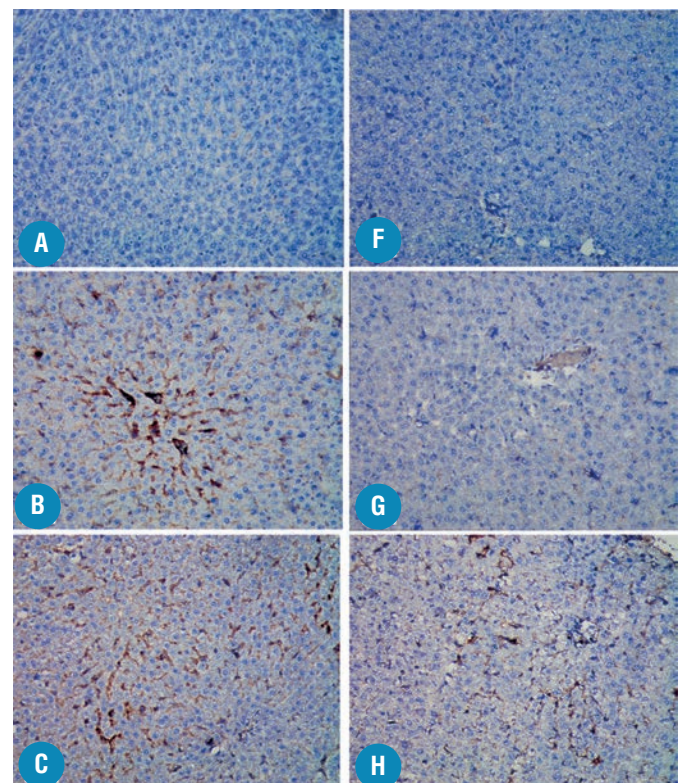
In addition, we performed an immunohistochemical staining of the liver sections to detect the presence of transforming growth factor-beta 1. TGF- β 1 is a cytokine that has been implicated in the development of liver fibrosis, a pathological process that can lead to cirrhosis and liver failure. It is expressed by various non-parenchymal cells, such as Kupffer cells, hepatic stellate cells (HSCs), liver sinusoidal endothelial cells, and dendritic cells, as well as by natural killer T cells and other hepatic lymphocytes. These cells are typically involved in the immune response and wound healing processes in the liver, and excessive and dysregulated TGF- β 1 production by these cells in response to injury contributes to liver fibrosis [37-40].

We found that TGF- β 1 was not expressed in the control and hUC-MSc control groups (**Fig. 2 A, F**) and less present in the groups treated with hUC-MSCs (**Fig. 2 G-J**) compared to the untreated ones (**Fig. 2 B-E**). Treatment at the earlier stage on the 14th day (**Fig. 2 I**) showed weaker staining compared to the later stage on the 21st day (**Fig. 2 J**), indicating reduced TGF- β 1 expression in the liver.

This finding suggests that hUC-MSCs have an antifibrotic effect by reducing the expression of TGF- β 1, which is known to cause the transformation of HSCs into myofibroblasts and stimulate the production of extracellular matrix proteins. Our results are consistent with previous animal studies using other types of MSCs, such as adipose-derived MSCs [41-42], hair follicle MSCs [43-44] and bone marrow-derived MSCs [45], which have demonstrated that MSCs can modulate the TGF- β 1 signaling pathway and inhibit liver fibrosis.

The degree of hepatocellular necrosis and inflammation was assessed and scored from 0 to 3 based on the severity of the lesion. The sum of the scores for each parameter was calculated to obtain a total histological score ranging from 0 to 18, with higher scores indicating more severe liver injury (**Table 1**).

The results indicate that LPS-induced liver injury in a time-dependent manner, with the highest scores observed at 28th day. Compared to the untreated groups, the groups treated with hUC-MSCs had a lower total histological score, indicating a potential therapeutic effect of hUC-MSCs on LPS-induced liver injury. Treatment with hUC-MSCs at an earlier stage (14th day) was more effective in reducing liver injury compared to treatment at a later stage (21st day). The control group and the group treated with hUC-MSCs alone showed no signs of liver injury.



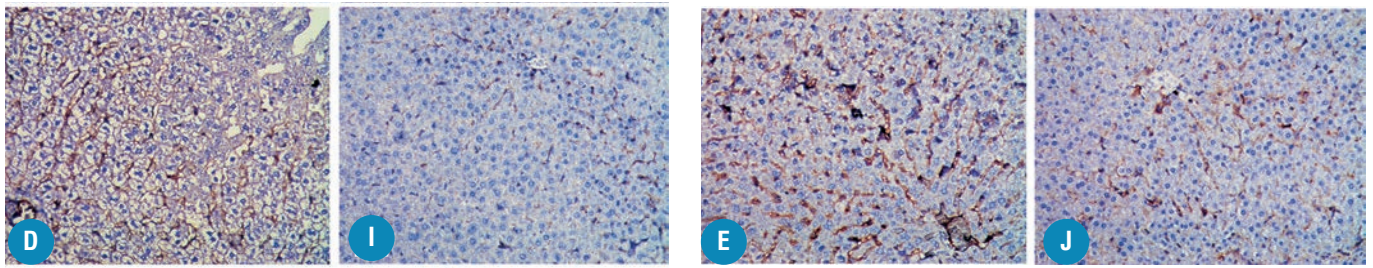


Fig. 2. Representative photomicrographs of rat liver sections stained for TGF-β1 by immunohistochemistry from control (A), 3d of LPS (B), 7d of LPS (C), 28d of LPS (D and E), control hUC-MSCs (F), 24h of LPS and 2d of hUC-MSCs (G), 4d of LPS and 3d of hUC-MSCs (H), 14d of LPS and 14d of hUC-MSCs (I), and 21d of LPS and 7d of hUC-MMSCs (J) groups. Sections counterstained with Mayer's hematoxylin; TGF-β1 staining is seen as a brown color. Images were captured at 200x magnification.

The liver enzymes alanine aminotransferase, aspartate aminotransferase, and alkaline phosphatase are important markers of liver injury. ALT and AST are primarily found within hepatocytes, and their levels in the blood increase when these cells are damaged. ALP, on the other hand, is

an enzyme found in the bile ducts and biliary epithelial cells and its levels rise in the presence of cholestasis or biliary obstruction [46-48]. The median values of AST, ALT and ALP are displayed in **Table 2**.

Table 1. Histological scoring of liver injury in experimental groups.

Group	Total histological Score	Hepatocellular necrosis	Liver structural damage	Hepatocyte vacuolation	Inflammation	DIC	TGF-β1 expression
Control	0	0	0	0	0	0	0
Control hUC-MSCs	0	0	0	0	0	0	0
3d LPS	11	1	2	1	2	3	2
7d LPS	12	2	2	1	2	3	2
28d LPS	15	3	3	3	1	2	3
24h LPS + 2d hUC-MSCs	3	0	1	0	1	0	1
4d LPS + 3d hUC-MSCs	4	1	0	0	1	0	2
14d LPS + 14d hUC-MSCs	3	0	1	0	1	0	1
21d LPS + 7d hUC-MSCs	7	1	1	1	1	1	2

Table 2. The median values of AST, ALT and ALP in the blood serum of experimental rats.

Group	AST (M, 25 %-75 %)	ALT (M, 25 %-75 %)	ALP (M, 25 %-75 %)
Control	98.4 (97.8; 101.7)	38.0 (37.7; 38.5)	216.0 (212.3; 221.0)
Control hUC-MSCs (3d)	100.9 (99.4; 103.4)	37.7 (37.2; 38.5)	214.8 (204.6; 222.1)
3d LPS	146.2 (142.3; 148.8)	44.2 (43.7; 45.1)	293.3 (283.1; 298.4)
7d LPS	166.2 (160.3; 170.9)	46.5 (45.7; 47.5)	297.6 (285.0; 309.9)
28d LPS	179.5 (174.0; 181.2)	47.1 (44.4; 48.9)	279.9 (274.4; 289.5)
24h LPS + 2d hUC-MSCs	113.9 (104.5; 124.5)	38.1 (37.9; 38.6)	229 (223.6; 233.5)
4d LPS + 3d hUC-MSCs	141.7 (136.7; 144.4)	44.2 (41.8; 45.6)	226.7 (219.5; 237.2)
14d LPS + 14d hUC-MSCs	103.9 (100.2; 104.9)	43.3 (42.3; 44.5)	250 (246.5; 253.6)
21d LPS + 7d hUC-MSCs	100.9 (99.9; 102.0)	43.9 (42.5; 44.7)	248.9 (235.9; 257.1)

Fig. 3 A displays the results of the AST measurements for the comparison group #1, **Fig. 3 B** displays the results for the comparison group #2, **Fig. 3 C** displays the results for the comparison group #3 in the form of box plots.

The comparisons of AST levels between different groups are presented in tables 3-5. When comparing the concentrations of AST, the level of significance was less than 0.05, indicating significant differences between the obtained data when comparing the concentrations in the following pairs of time points: control – 3d; control – 7d; control – 28d; control – 24h + 2d hUC-MSCs; control – 4d + 3d hUC-MSCs; 3d – 24h + 2d hUC-MSCs; 7d – 4d + 3d hUC-MSCs; 28d – 14d + 14d hUC-MSCs; 28d – 21d + 7d hUC-MSCs; 7d – control hUC-MSCs; 4d + 3d hUC-MSCs – control hUC-MSCs.

When comparing data taken at the time points control – control hUC-MSCs; control – 14d + 14d hUC-MSCs; control – 21d + 7d hUC-MSCs; 14d + 14d hUC-MSCs – 21d + 7d hUC-MSCs; which is greater than 0.05. This indicates the absence of significant differences in AST concentrations between these data points.

Fig. 4 A displays the results of the ALT measurements for the comparison group #1, **Fig. 4 B** displays the results for the comparison group #2, **Fig. 4 C** displays the results for the comparison group #3 in the form of box plots.

The comparisons of ALT levels between different groups are presented in tables 6-8. When comparing the concentrations of ALT, the level of significance was less than 0.05, indicating significant differences between the obtained data when comparing the concentrations in the following pairs of time points: control – 3d; control – 7d; control – 28d; control – 4d + 3d hUC-MSCs; control – 14d + 14d hUC-MSCs; control – 21d + 7d hUC-MSCs; 3d – 24h + 2d hUC-MSCs; 7d – 4d + 3d hUC-MSCs; 28d – 14d + 14d hUC-MSCs; 28d – 21d + 7d hUC-MSCs; 7d – control hUC-MSCs; 4d + 3d hUC-MSCs – control hUC-MSCs.

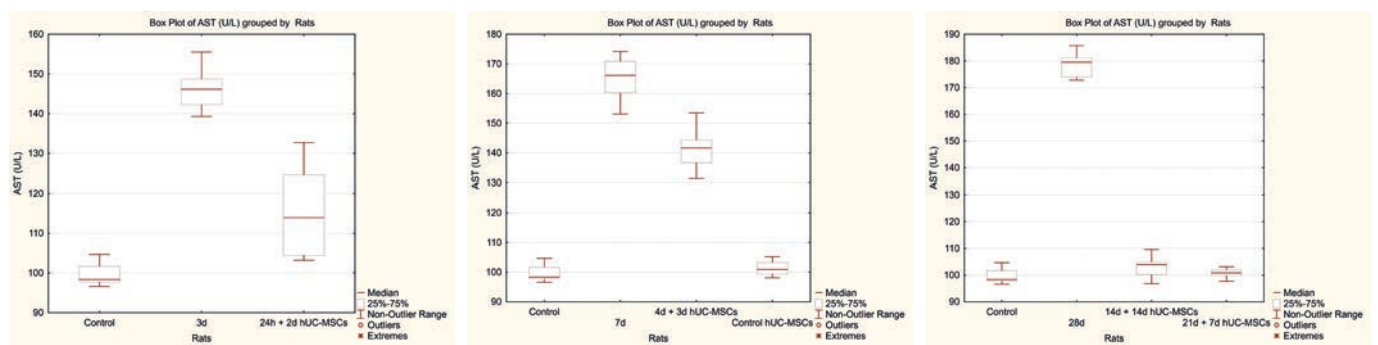


Fig. 3. Levels of AST in rat blood serum after LPS administration and the treatment with hUC-MSCs at different time points in U/L. A – comparison group #1, B – comparison group #2; C – comparison group #3. Statistically significant differences between groups are presented in tables 3-5.

Table 3. Differences in AST levels in comparison group #1.

AST	Control	3d	24h + 2d hUC-MSCs
Control	X	(p = 0.0008)	(p = 0.0023)
3d	(p = 0.0008)	X	(p = 0.0008)
24h + 2d hUC-MSCs	(p = 0.0023)	(p = 0.0008)	X

Note: «+» indicates the presence of statistically significant difference between groups.

Table 4. Differences in AST levels in comparison group #2.

AST	Control	7d	4d + 3d hUC-MSCs	Control hUC-MSCs
Control	X	(p = 0.0008)	(p = 0.0023)	(p = 0.1415)
7d	(p = 0.0008)	X	(p = 0.0011)	(p = 0.0008)
4d + 3d hUC-MSCs	(p = 0.0023)	p = 0.0011	X	(p = 0.0008)
Control hUC-MSCs	(p = 0.1415)	(p = 0.0008)	(p = 0.0008)	X

Note: «+» indicates the presence of statistically significant difference between groups; «-» indicates the absence of statistically significant difference.

Table 5. Differences in AST levels in comparison group #3.

AST	Control	28d	14d + 14d hUC-MSCs	21d + 7d hUC-MSCs
Control	X	(p = 0.0008)	(p = 0.1152)	(p = 0.2698)
28d	(p = 0.0008)	X	(p = 0.0008)	(p = 0.0008)
14d + 14d hUC-MSCs	(p = 0.1152)	(p = 0.0008)	X	(p = 0.1152)
21d + 7d hUC-MSCs	(p = 0.2698)	(p = 0.0008)	(p = 0.1152)	X

Note: «+» indicates the presence of statistically significant difference between groups; «-» indicates the absence of statistically significant difference.

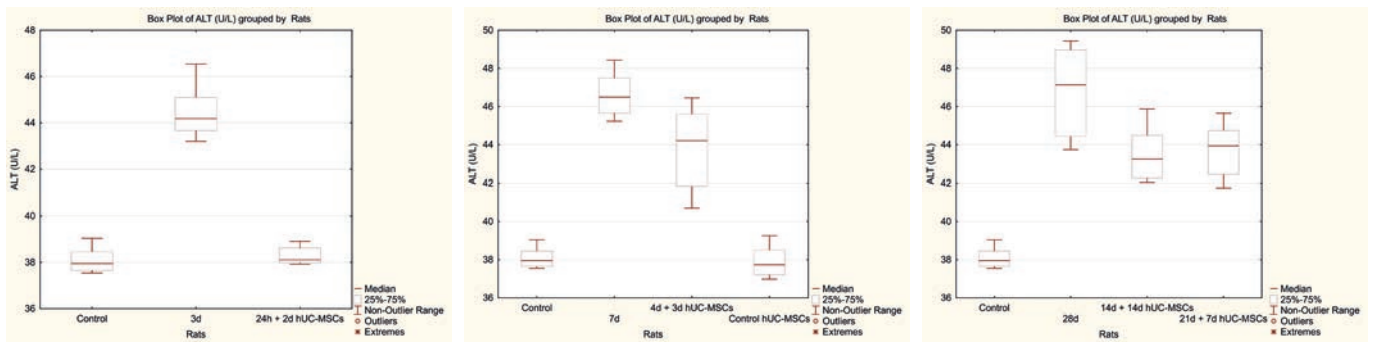


Fig. 4. Levels of ALT in rat blood serum after LPS administration and the treatment with hUC-MSCs at different time points in U/L. A – comparison group #1, B - comparison group #2; C – comparison group #3. Statistically significant differences between groups are presented in tables 6-8.

Table 6. Differences in ALT levels in comparison group #1.

AST	Control	3d	24h + 2d hUC-MSCs
Control	X	+ (p = 0.0008)	- (p = 0.2473)
3d	+ (p = 0.0008)	X	+ (p = 0.0008)
24h + 2d hUC-MSCs	- (p = 0.2473)	+ (p = 0.0008)	X

Note: «+» indicates the presence of statistically significant difference between groups; «-» indicates the absence of statistically significant difference.

Table 7. Differences in ALT levels in comparison group #2.

AST	Control	7d	4d + 3d hUC-MSCs	Control hUC-MSCs
Control	X	+ (p = 0.0008)	+ (p = 0.0008)	- (p = 0.4623)
7d	+ (p = 0.0008)	X	+ (p = 0.0117)	+ (p = 0.0008)
4d + 3d hUC-MSCs	+ (p = 0.0008)	+ (p = 0.0117)	X	+ (p = 0.0008)
Control hUC-MSCs	- (p = 0.4623)	+ (p = 0.0008)	+ (p = 0.0008)	X

Note: «+» indicates the presence of statistically significant difference between groups; «-» indicates the absence of statistically significant difference.

Table 8. Differences in ALT levels in comparison group #3.

AST	Control	28d	14d + 14d hUC-MSCs	21d + 7d hUC-MSCs
Control	X	+ (p = 0.0008)	+ (p = 0.0008)	+ (p = 0.0008)
28d	+ (p = 0.0008)	X	+ (p = 0.0117)	+ (p = 0.0209)
14d + 14d hUC-MSCs	+ (p = 0.0008)	+ (p = 0.0117)	X	- (p = 0.7527)
21d + 7d hUC-MSCs	+ (p = 0.0008)	+ (p = 0.0209)	- (p = 0.7527)	X

Note: «+» indicates the presence of statistically significant difference between groups; «-» indicates the absence of statistically significant difference.

When comparing data taken at the time points control – control hUC-MSCs; control – 24h + 2d hUC-MSCs; 14d + 14d hUC-MSCs – 21d + 7d hUC-MSCs, which is greater than 0.05. This indicates the absence of significant differences in ALT concentrations between these data points.

Fig. 5 A displays the results of the ALP measurements for the comparison group #1, Fig. 5 B displays the results for the comparison group #2, Fig. 5 C displays the results for the comparison group #3 in the form of box plots.

When comparing the concentrations of ALP, the level of significance was less than 0.05, indicating significant differences between the obtained data when comparing the concentrations in the following pairs of time points: control – 3d; control – 7d; control - 28d; control – 24h + 2d hUC-MSCs; control – 4d + 3d hUC-MSCs; control – 14d + 14d hUC-MSCs; control – 21d + 7d hUC-MSCs; 3d – 24h + 2d hUC-MSCs; 7d – 4d + 3d hUC-MSCs; 28d – 14d + 14d hUC-MSCs; 28 days – 21d + 7d hUC-MSCs; 7d – control hUC-MSCs; 4d + 3d hUC-MSCs – control hUC-MSCs.

When comparing data taken at the time points control – control hUC-MSCs; 14d + 14d hUC-MSCs – 21d + 7d hUC-MSCs; which is greater than 0.05. This indicates the absence of significant differences in ALP concentrations between these data points.

Summarizing the obtained results, it can be concluded that the levels of ALT, AST, and ALP were significantly elevated in the blood serum of untreated rats. These results suggest that the liver cells were damaged and the hepatic function was impaired. In contrast, the levels of these liver markers were lower in the rats treated with hUC-MSCs, indicating that the treatment was effective in reducing hepatocellular damage.

These results are consistent with previous studies that have demonstrated the potential of hUC-MSCs therapy in various animal models of liver injury [49; 50], as well as in clinical trials [51]. The beneficial effects of hUC-MSCs treatment are thought to be mediated through multiple mechanisms, including the ability of these cells to modulate the immune response, reduce oxidative stress and inflammation, promote tissue repair and regeneration as well as inhibit fibrosis [52-55].

Zhang et al. evaluated the therapeutic effect of hUC-MSCs at various passages on acute liver failure in rats. The results showed that hUC-MSCs transplantation enhanced the regeneration and inhibited the apoptosis of

hepatocytes in rats with acute liver failure. Moreover, the therapeutic effect of hUC-MSCs was better at passage 5 compared to passage 10 [56].

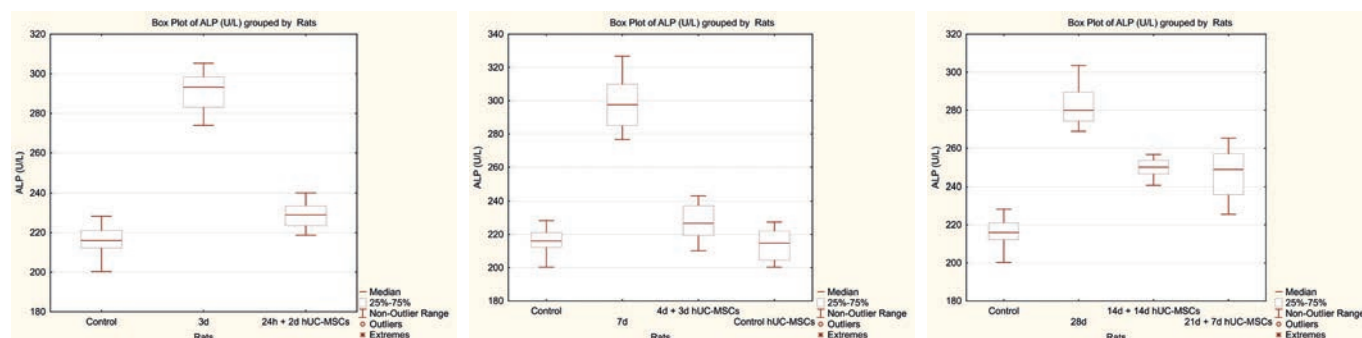


Fig. 5. Levels of ALP in rat blood serum after LPS administration and the treatment with hUC-MSCs at different time points in U/L. A – comparison group #1, B - comparison group #2; C – comparison group #3. Statistically significant differences between groups are presented in tables 9-11.

THE COMPARISONS OF ALP LEVELS BETWEEN DIFFERENT GROUPS ARE PRESENTED IN TABLES 9-11

Table 9. Differences in ALP levels in comparison group #1.

AST	Control	3d	24h + 2d hUC-MSCs
Control	X	+ (p = 0.0008)	+ (p = 0.0063)
3d	+ (p = 0.0008)	X	+ (p = 0.0008)
24h + 2d hUC-MSCs	+ (p = 0.0063)	+ (p = 0.0008)	X

Note: «+» indicates the presence of statistically significant difference between groups.

Table 10. Differences in ALP levels in comparison group #2.

AST	Control	7d	4d + 3d hUC-MSCs	Control hUC-MSCs
Control	X	+ (p = 0.0008)	+ (p = 0.0404)	- (p = 0.7130)
7d	+ (p = 0.0008)	X	+ (p = 0.0008)	+ (p = 0.0008)
4d + 3d hUC-MSCs	+ (p = 0.0404)	+ (p = 0.0008)	X	+ (p = 0.0357)
Control hUC-MSCs	- (p = 0.7130)	+ (p = 0.0008)	+ (p = 0.0357)	X

Note: «+» indicates the presence of statistically significant difference between groups; «-» indicates the absence of statistically significant difference.

Table 11. Differences in ALP levels in comparison group #3.

AST	Control	28d	14d + 14d hUC-MSCs	21d + 7d hUC-MSCs
Control	X	+ (p = 0.0008)	+ (p = 0.0008)	+ (p = 0.0011)
28d	+ (p = 0.0008)	X	+ (p = 0.0008)	+ (p = 0.0008)
14d + 14d hUC-MSCs	+ (p = 0.0008)	+ (p = 0.0008)	X	- (p = 0.8336)
21d + 7d hUC-MSCs	+ (p = 0.0011)	+ (p = 0.0008)	- (p = 0.8336)	X

Note: «+» indicates the presence of statistically significant difference between groups; «-» indicates the absence of statistically significant difference.

Huang et al. report on the therapeutic effects of MSCs and their secreted molecules on two different models of liver disease in mice. According to the study, MSCs showed potential for treating fulminant hepatic failure through immunosuppression and promotion of survival via interaction with various inflammation-related cells, while its conditioned medium exhibited potential for treating chronic liver fibrosis through down-regulation of inflammatory responses and promotion of HSCs apoptosis [57].

Cai et al. in their study aimed to investigate the potential of bone marrow-derived mesenchymal stem cells (BM-MSCs) in inhibiting hepa-

toocyte apoptosis after acute liver injury in a rat model. The results showed that BM-MSCs transplantation increased the levels of anti-inflammatory cytokines and reduced hepatocyte apoptosis [58].

Ayatollahi et al. investigated the antioxidant effects of BM-MSCs against carbon tetrachloride-induced oxidative damage in rat livers. The results showed that BM-MSCs significantly suppressed the oxidative stress and increased the activity of antioxidant enzymes indicating their potential therapeutic use in liver diseases associated with oxidative stress [60].

Ryu et al. investigated the potential therapeutic effects of tonsil-derived mesenchymal stem cells (T-MSCs) on concanavalin A-induced acute liver injury in mice. The results showed that T-MSCs reduced liver damage and decreased pro-inflammatory cytokine expression [59].

In the context of ARDS-induced liver injury, MSCs have been found to have additional benefits, such as reducing lung inflammation and improving lung function. This is likely due to the cross-talk between the liver and the lungs, as both organs are affected by ARDS [61-63].

CONCLUSION

In summary, our findings suggest that hUC-MSCs have regenerative, anti-inflammatory, and antifibrotic effects on LPS-induced liver injury. The severity of parenchymal destruction in the liver increases with the duration of time after LPS exposure. The regenerative effect of hUC-MSCs was found to be greater in the group 14d LPS + 14d hUC-MSCs compared to the group 21d LPS + 7d hUC-MSCs. These findings suggest that the administration of hUC-MSCs at an earlier time point (14 days) enhances their regenerative potential.

Overall, our study adds to the growing body of evidence supporting the therapeutic potential of hUC-MSCs in liver injury, and highlights the advantages of these cells as a promising source for cell-based therapy.

FUNDING

The study was supported by the Ministry of Health of Ukraine as a part of the state-funded research work “Investigation of the regenerative potential of cellular therapy agents in acute respiratory distress syndrome” (2021-2023, state registration number 0121U100159).

REFERENCES:

- Shyamala V, Harini R, Manikandan D, Riyaz SM. Acute Respiratory Distress Syndrome (ARDS). In: An Epidemiological Update on COVID-19. 2022: 1-9. Doi: 10.2174/9789815050325122010005
- Huppert LA, Matthay MA, Ware LB. Pathogenesis of acute respiratory distress syndrome. *Semin Respir Crit Care Med.* 2019; 40(1):31-39. Available from: <https://doi.org/10.1055/s-0039-1683996>
- Michael AM, Zemans RL, Zimmerman GA, et al. Acute respiratory distress syndrome. *Nat Rev Dis Primers.* 2019; 5:18. Available from: <https://doi.org/10.1038/s41572-019-0069-0>
- Thompson BT, Chambers RC, Liu KD. Acute respiratory distress syndrome. *N Engl J Med.* 2017; 377:562-72. Available from: <https://doi.org/10.1056/NEJMra1608077>
- Bellani G, Laffey JG, Pham T, Fan E, Brochard L, Esteban A, et al. Epidemiology, patterns of care, and mortality for patients with acute respiratory distress syndrome in intensive care units in 50 countries. *Jama.* 2016; 315(8): 788-800. Available from: <https://doi.org/10.1001/jama.2016.0291>
- Herrero R, Sánchez G, Asensio I, López E, et al. Liver-lung interactions in acute respiratory distress syndrome. *Intensive Care Med Exp.* 2020; 8(1):1-13. Available from: <https://doi.org/10.1186/s40635-020-00337-9>
- Kallet RH, Lipnick MS, Zhuo H, Pangilinan LP, Gomez A. Characteristics of nonpulmonary organ dysfunction at onset of ARDS based on the Berlin definition. 2019. Available from: <https://doi.org/10.4187/respcare.06165>
- Dawood RM, Salum GM, Abd El-Meguid M. The impact of COVID-19 on liver injury. *The American Journal of the Medical Sciences.* 2022; 363(2):94-103. Available from: <https://doi.org/10.1016/j.amjms.2021.11.001>
- Harnisch, LO, Baumann S, Mihaylov D, Kiehntopf M, Bauer M, Moerer O, et al. Biomarkers of cholestasis and liver injury in the early phase of acute respiratory distress syndrome and their pathophysiological value. *Diagnostics.* 2021; 11(12): 2356. Available from: <https://doi.org/10.3390/diagnostics11122356>
- Guillot A, Tacke F. Liver macrophages: old dogmas and new insights. *Hepatology communications.* 2019; 3(6):730-743. Available from: <https://doi.org/10.1002/hep4.1356>
- Weber M, Lambeck S, Ding N, Henken S, Kohl M, Deigner HP, et al. Hepatic induction of cholesterol biosynthesis reflects a remote adaptive response to pneumococcal pneumonia. *The FASEB Journal.* 2012; 26(6):2424-2436. Available from: <https://doi.org/10.1096/fj.11-191957>
- Quinton LJ, Blahna MT, Jones MR, Allen E, Ferrari JD, Hilliard KL, et al. Hepatocyte-specific mutation of both NF- κ B RelA and STAT3 abrogates the acute phase response in mice. *J Clin Invest.* 2012; 122(5):1758-1763. Available from: <https://doi.org/10.1172/JCI59408>
- Dickson RP. The lung microbiome and ARDS. It is time to broaden the model. 2018. Available from: <https://doi.org/10.1164/rccm.201710-2096ED>
- Dickson RP, Singer BH, Newstead MW, Falkowski NR, Erb-Downward JR, Standiford TJ, et al. Enrichment of the lung microbiome with gut bacteria in sepsis and the acute respiratory distress syndrome. *Nat Microbiol.* 2016; 1(10):1-9. Available from: <https://doi.org/10.1038/nmicrobiol.2016.113>
- de Jong PR, González-Navajas JM, Jansen NJG. The digestive tract as the origin of systemic inflammation. *Crit Care.* 2016; 20(1):1-12. Available from: <https://doi.org/10.1186/s13054-016-1458-3>

16. Massey VL, Poole LG, Siow DL, Torres E, Warner NL, Schmidt RH, et al. Chronic Alcohol Exposure Enhances Lipopolysaccharide — Induced Lung Injury in Mice: Potential Role of Systemic Tumor Necrosis Factor-Alpha. *Alcohol Clin Exp Res*. 2015; 39(10):1978-1988. Available from: <https://doi.org/10.1111/acer.12855>
17. Massey VL. Potential role of the gut/liver/lung axis in alcohol-induced tissue pathology. *Biomolecule*. 2015; 5(4):2477-2503. Available from: <https://doi.org/10.3390/biom504247718>.
18. Domscheit H, Hegeman MA, Carvalho N, Spieth PM. Molecular dynamics of lipopolysaccharide-induced lung injury in rodents. *Front Physiol*. 2020; 11:36. Available from: <https://doi.org/10.3389/fphys.2020.00036>
19. George T, Chakraborty M, Gienbycz MA, Newton R. A bronchoprotective role for Rgs2 in a murine model of lipopolysaccharide-induced airways inflammation. *Allergy Asthma Clin Immunol*. 2018; 14(1):1-14. Available from: <https://doi.org/10.1186/s13223-018-0266-5>
20. de Souza Xavier Costa N, Ribeiro Júnior G, dos Santos Alemany AA, Belotti L, Zati DH, Frota Cavalcante M, et al. Early and late pulmonary effects of nebulized LPS in mice: An acute lung injury model. *PLoS One*. 2017; 12(9):e0185474. Available from: <https://doi.org/10.1371/journal.pone.0185474>
21. Barnett-Vanes A, Sharrock A, Birrell MA, Rankin S. A single 9-colour flow cytometric method to characterise major leukocyte populations in the rat: validation in a model of LPS-induced pulmonary inflammation. *PLoS One*. 2016; 11(1):e0142520. Available from: <https://doi.org/10.1371/journal.pone.0142520>
22. Roos AB, Berg T, Ahlgren KM, Grunewald J, Nord M. A method for generating pulmonary neutrophilia using aerosolized lipopolysaccharide. *J Vis Exp*. 2014; (94):e51470. Available from: <https://doi.org/10.3791/51470>
23. Fan X, Li L, Ye Z, Zhou Y, Tan WS, Yang J. Advances in umbilical cord mesenchymal stem cells: A review of their potential in regenerative medicine. *Expert Opin Biol Ther*. 2021; 21(10):1355-1366. Available from: <https://doi.org/10.1080/14712598.2021.1921837>
24. Redko O, Dovgalyuk A, Dovbush A, Nebesna Z, Yakubyshyna L, Krynyska I. Liver injury associated with acute respiratory distress syndrome and the prospects of mesenchymal stem cells therapy for liver failure. *Cell Organ Transpl*. 2021; 9(2):136-142. Available from: <https://doi.org/10.22494/cot.v9i2.13025>
25. Wang M, Yuan Q, Xie L. Mesenchymal stem cell-based immunomodulation: properties and clinical application. *Stem Cells Int*. 2018; 2018:3057624. Available from: <https://doi.org/10.1155/2018/3057624>
26. Ankrum JA, Ong JF, Karp JM. Mesenchymal stem cells: immune evasive, not immune privileged. *Nat Biotechnol*. 2014; 32(3):252-260. Available from: <https://doi.org/10.1038/nbt.2816>
27. Fröhlich E. Acute Respiratory Distress Syndrome: Focus on Viral Origin and Role of Pulmonary Lymphatics. *Biomedicines*. 2021; 9(11):1732. Available from: <https://doi.org/10.3390/biomedicines9111732>
28. Krynyska I, Marushchak M, Birchenko I, Dovgalyuk A, Tokarsky O. COVID-19-associated acute respiratory distress syndrome versus classical acute respiratory distress syndrome (a narrative review). *Iran J Microbiol*. 2021; 13(6):728-738. Available from: <https://doi.org/10.18502/ijm.v13i6.8072>
29. Strassmair M. Alpha-1-Antitrypsin expressing Mesenchymal Stem Cells (MSC-AAT) for the treatment of severe cases of COVID-19 infection. 2020. Available from: https://www.academia.edu/44792707/Alpha_1_Antitrypsin_expressing_Mesenchymal_Stem_Cells_MSC_AAT_for_the_treatment_of_severe_cases_of_COVID_19_infection
30. Iglesias M, Butrón P, Torre-Villalvazo I, Torre-Anaya EA, Sierra-Madero J, Rodriguez-Andoney JJ, et al. Mesenchymal stem cells for the compassionate treatment of severe acute respiratory distress syndrome due to COVID-19. *Aging Dis*. 2021; 12(2):360. Available from: <https://doi.org/10.14336/AD.2020.1218>
31. Leng Z, Zhu R, Hou W, Feng Y, Yang Y, Han Q, et al. Transplantation of ACE2-mesenchymal stem cells improves the outcome of patients with COVID-19 pneumonia. *Aging and disease*. 2020; 11(2):216. Available from: <https://doi.org/10.14336/AD.2020.0228>
32. Wilson JG, Liu KD, Zhuo H, Caballero L, McMillan M, Fang X, et al. Mesenchymal stem (stromal) cells for treatment of ARDS: a phase 1 clinical trial. *The Lancet Respiratory Medicine*. 2015; 3(1):24-32. Available from: [https://doi.org/10.1016/S2213-2600\(14\)70291-7](https://doi.org/10.1016/S2213-2600(14)70291-7)
33. Sanchez-Diaz M, Quiñones-Vico MI, Sanabria de la Torre R, Montero-Vilchez T, Sierra-Sánchez A, Molina-Leyva A, et al. Biodistribution of mesenchymal stromal cells after administration in animal models and humans: a systematic review. *J Clin Med*. 2021; 10(13):2925. Available from: <https://doi.org/10.3390/jcm10132925>
34. Livingstone SA, Wildi KS, Dalton HJ, Usman A, Ki KK, Passmore, MR, et al. Coagulation Dysfunction in Acute Respiratory Distress Syndrome and Its Potential Impact in Inflammatory Subphenotypes. *Front Med*. 2021; 8: 723217. Available from: <https://doi.org/10.3389/fmed.2021.723217>
35. Gando S, Fujishima S, Saitoh D, Shiraishi A, Yamakawa K, Kushimoto S, et al. The significance of disseminated intravascular coagulation on multiple organ dysfunction during the early stage of acute respiratory distress syndrome. *Thromb Res*. 2020; 191: 15-21. Available from: <https://doi.org/10.1016/j.thromres.2020.03.023>
36. Chang JC. Acute respiratory distress syndrome as an organ phenotype of vascular microthrombotic disease: based on hemostatic theory and endothelial molecular pathogenesis. *Clinical and Applied Thrombosis/Hemostasis*, 2019; 25: 1076029619887437. Available from: <https://doi.org/10.1177/1076029619887437>
37. Higashi T, Friedman SL, Hoshida Y. Hepatic stellate cells as key target in liver fibrosis. *Adv Drug Deliv Rev*. 2017; 121:27-42. Available from: <https://doi.org/10.1016/j.addr.2017.05.007>
38. Pellicoro A, Ramachandran P, Iredale JP, Fallowfield JA. Liver fibrosis and repair: immune regulation of wound healing in a solid organ. *Nat Rev Immunol*. 2014; 14:181-194. Available from: <https://doi.org/10.1038/nri3623>
39. Schon HT, Weiskirchen R. Immunomodulatory effects of transforming growth factor- β in the liver. *Hepatobiliary Surg Nutr*. 2014; 3(6):386-406. Available from: <https://doi.org/10.3978/j.issn.2304-3881.2014.11.06>
40. Dooley S, Ten Dijke P. TGF- β in progression of liver disease. *Cell and tissue research*. 2012; 347(1):245-256. Available from: <https://doi.org/10.1007/s00441-011-1246-y>
41. Yang N, Ma W, Ke Y, Liu H, Chu J, Sun L, et al. Transplantation of adipose-derived stem cells ameliorates Echinococcus multilocularis-induced liver fibrosis in mice. *PLoS Neglected Tropical Diseases*. 2022; 16(1):e0010175. Available from: <https://doi.org/10.1371/journal.pntd.0010175>
42. Fathy M, Okabe M, Saad Eldien HM, Yoshida T. AT-MSCs antifibrotic activity is improved by eugenol through modulation of TGF- β /Smad signaling pathway in rats. *Molecules*. 2020; 25(2):348. Available from: <https://doi.org/10.3390/molecules25020348>
43. Liu Q, Lv C, Jiang Y, Luo K, Gao Y, Liu J, et al. From hair to liver: Emerging application of hair follicle mesenchymal stem cell transplantation reverses liver cirrhosis by blocking the TGF- β /Smad signaling pathway to inhibit pathological HSC activation. *Peer J*. 2022; 10:e12872. Available from: <https://doi.org/10.7717/peerj.12872>
44. Liu Q, Lv C, Huang Q, et al. ECM1 modified HF-MSCs targeting HSC attenuate liver cirrhosis by inhibiting the TGF- β /Smad signaling pathway. *Cell Death Discovery*. 2022; 8(1):51. Available from: <https://doi.org/10.1038/s41420-022-00846-4>
45. Jang YO, Kim SH, Cho MY, Kim KS, Park KS, Cha SK, et al. Synergistic effects of simvastatin and bone marrow-derived mesenchymal stem cells on hepatic fibrosis. *Biochemical and biophysical research communications*. 2018; 497(1):264-71. Available from: <https://doi.org/10.1016/j.bbrc.2017.12.091>
46. McGill MR. The past and present of serum aminotransferases and the future of liver injury biomarkers. *EXCLI J*. 2016; 15:817. Available from: <https://doi.org/10.17179/excli2016-800>
47. Levick C. How to interpret liver function tests. *South Sudan Med J*. 2017; 10(2):40-43.
48. Moriles K, Azer S. Alanine Amino Transferase. 2022. Available from: <https://www.ncbi.nlm.nih.gov/books/NBK559278>
49. Wang CH, Chen CY, Wang KH, Kao AP, Chen YJ, Lin PH, et al. Comparing the Therapeutic Mechanism and Immune Response of Human and Mouse Mesenchymal Stem Cells in Immunocompetent Mice With Acute Liver Failure. *Stem Cells Transl Med*. 2023. Available from: <https://doi.org/10.1093/stcltm/szac084>

50. Hu C, Wu Z, Li L. Pre-treatments enhance the therapeutic effects of mesenchymal stem cells in liver diseases. *JCMM*. 2020; 24(1):40-49. Available from: <https://doi.org/10.1111/jcmm.14788>
51. Tsuchiya A, Kojima Y, Ikarashi S, Seino S, Watanabe Y, Kawata Y, et al. Clinical trials using mesenchymal stem cells in liver diseases and inflammatory bowel diseases. *Inflamm Regen*. 2017; 37(1): 1-15. Available from: <https://doi.org/10.1186/s41232-017-0045-6>
52. Kang H, Kim MY, Eom YW, Baik SK. Mesenchymal stem cells for the treatment of liver disease: present and perspectives. *Gut Liver*. 2020; 14(3):306. Available from: <https://doi.org/10.5009/gnl18412>
53. Wang YH, Wu DB, Chen B, Chen EQ, Tang H. Progress in mesenchymal stem cell-based therapy for acute liver failure. *Stem Cell Res Therapy*. 2018; 9(1):1-9. Available from: <https://doi.org/10.1186/s13287-018-0972-4>
54. Wang J, Cen P, Chen J, Fan L, Li J, Cao H, et al. Role of mesenchymal stem cells, their derived factors, and extracellular vesicles in liver failure. *Stem Cell Res Ther*. 2017; 8:137. Available from: <https://doi.org/10.1186/s13287-017-0576-4>
55. Gazdic M, Arsenijevic A, Markovic BS, Volarevic A, Dimova I, Djonov V, et al. Mesenchymal stem cell-dependent modulation of liver diseases. *Int J Biol Sci*. 2017; 13(9):1109. Available from: <https://doi.org/10.7150/ijbs.20240>
56. Zhang Y, Li Y, Li W, Cai J, Yue M, Jiang L, et al. Therapeutic effect of human umbilical cord mesenchymal stem cells at various passages on acute liver failure in rats. *Stem Cells Int*. 2018; 2018. Available from: <https://doi.org/10.1155/2018/7159465>
57. Huang B, Cheng X, Wang H, et al. Mesenchymal stem cells and their secreted molecules predominantly ameliorate fulminant hepatic failure and chronic liver fibrosis in mice respectively. *J Transl Med*. 2016; 14:45. Available from: <https://doi.org/10.1186/s12967-016-0792-1>
58. Cai Y, Zou Z, Liu L, Chen S, Chen Y, Lin Z, et al. Bone marrow-derived mesenchymal stem cells inhibits hepatocyte apoptosis after acute liver injury. *Int J Clin Exp*. 2015; 8(1): 107-16.
59. Ryu KH, Kim SY, Kim YR, et al. Tonsil-derived mesenchymal stem cells alleviate concanavalin A-induced acute liver injury. *Exp Cell Res*. 2014; 326:143-154. Available from: <https://doi.org/10.1016/j.yexcr.2014.06.007>
60. Ayatollahi M, Hesami Z, Jamshidzadeh A, Gramizadeh B. Antioxidant effects of bone marrow mesenchymal stem cell against carbon tetrachloride-induced oxidative damage in rat livers. *Int J Organ Transplant Med*. 2014; 5(4):166-73.
61. Xu J, Qu J, Cao L, Sai Y, Chen C, He L, et al. Mesenchymal stem cell-based therapy for acute respiratory distress syndrome: from basic to clinics. *Protein Cell*. 2019; 10(10):710-727. Available from: <https://doi.org/10.1007/s13238-019-0643-3>
62. Silva JD, Lopes-Pacheco M, Paz AH, Cruz FF, Melo EB, de Oliveira MV, et al. Mesenchymal stem cells from bone marrow, adipose tissue, and lung tissue differentially mitigate lung and distal organ damage in experimental acute respiratory distress syndrome. *Crit Care Med*. 2018; 46(2):e132-e140. Available from: <https://doi.org/10.1097/CCM.0000000000002848>
63. Mokhber Dezfouli MR, Jabbari Fakhri M, Sadeghian Chaleshtori S, Dehghan MM, Vajhi A, Mokhtari R. Intrapulmonary autologous transplant of bone marrow-derived mesenchymal stromal cells improves lipopolysaccharide-induced acute respiratory distress syndrome in rabbit. *Crit Care Med*. 2018; 22:1-13. Available from: <https://doi.org/10.1186/s13054-018-2272-x>



ARTICLE ON THE SITE
[TRANSPLANTOLOGY.ORG](https://www.transplantology.org)

The authors declare that there is no potential conflict of interest regarding the research, authorship and/or publication of this article.

УДК: 616.36:616.24-008.64-085.36-092.9

Мезенхімальні стромальні клітини пуповини людини зменшують наслідки індукованого ліпополісахаридом пошкодження печінки у щурів



Редько О. С., Довгалюк А. І., Крамар С. Б., Небесна З. М., Сверстюк А. С., Корда М. М.

Тернопільський національний медичний університет імені І. Я. Горбачевського МОЗ України, Тернопіль, Україна

РЕЗЮМЕ

Гострий респіраторний дистрес-синдром – це важкий клінічний стан, який здатний спричинити поліорганну недостатність, включаючи ураження печінки. Показано, що мезенхімальні стромальні клітини (МСК) пуповини людини проявляють терапевтичний потенціал щодо низки хвороб завдяки своїй здатності диференціюватися у різні типи клітин, а також своїм протизапальним та імуномодуляторним властивостям.

МЕТА ДОСЛІДЖЕННЯ: встановити потенціал МСК пуповини людини у лікуванні ураження печінки щурів, викликаного ліпополісахаридом (ЛПС).

МАТЕРІАЛИ ТА МЕТОДИ. Зрілі щурі-самці лінії Wistar були випадковим чином розподілені на 9 груп: контроль, 3 дні, 7 днів та 28 днів після інтраназального введення ЛПС, 24 години ЛПС і 2 дні МСК, 4 дні ЛПС і 3 дні МСК, 14 днів ЛПС і 14 днів МСК, 21 день ЛПС і 7 днів МСК і контроль 3 дні після введення МСК. Ізоляція МСК із тканини пуповини людини була проведена за допомогою ферментативного методу з використанням колагенази I. МСК вводили інтраперитонеально у дозі $1 \cdot 10^6$ клітин/кг маси тіла. Сироваткові рівні аланінаміно-трансферази (АЛТ), аспартатаміно-трансферази (АСТ) та лужної фосфатази (ЛФ) вимірювали кінетичним методом. Рівні гепатоцелюлярного некрозу, ураження структури печінки, вакуолізації гепатоцитів, запалення та дисемінованого внутрішньосудинного зсідання крові (ДВЗ) визначали за допомогою гістологічного аналізу зрізів, забарвлених гематоксиліном-еозином. Експресію TGF- β 1 у тканинах печінки оцінювали імуногістохімічним методом.

РЕЗУЛЬТАТИ. Доклінічне дослідження продемонструвало, що терапія з використанням МСК пуповини людини значно покращує функцію печінки і знижує ЛПС-індуковане ураження печінки у щурів. Про це свідчило зменшення гепатоцелюлярного некрозу, ураження структури печінки, вакуолізації гепатоцитів, запалення, ознак ДВЗ, фіброзу та зниження рівнів сироваткових маркерів печінки АЛТ, АСТ та ЛФ у групах, пролікованих МСК у порівнянні з нелікованими групами. Дослідження також виявило, що застосування МСК було більш ефективним на більш ранній стадії ураження печінки.

ВИСНОВКИ. Наші результати свідчать, що терапія з використанням МСК пуповини людини має потенціал для лікування ЛПС-індукованого ураження печінки. Подальші дослідження потрібні для того, щоб краще зрозуміти основні механізми та визначити потенціал клітинної терапії у клінічній практиці.

КЛЮЧОВІ СЛОВА: ураження печінки; мезенхімальні стромальні клітини пуповини людини; клітинна терапія; гістологічний аналіз